Vietnam Journal of Mechanics, VAST, Vol. 40, No. 3 (2018), pp. 243 – 250
DOI: https://doi.org/10.15625/0866-7136/10982

ATOMISTIC SIMULATION OF THE UNIAXIAL COMPRESSION OF BLACK PHOSPHORENE NANOTUBES

Van-Trang Nguyen[1,2], **Minh-Quy Le**[1,*]
[1]*Hanoi University of Science and Technology, Vietnam*
[2]*Thai Nguyen University of Technology, Thai Nguyen city, Vietnam*
[*]E-mail: quy.leminh@hust.edu.vn
Received December 15, 2017

Abstract. We study through molecular dynamics finite element method with Stillinger–Weber potential the uniaxial compression of (0, 24) armchair and (31, 0) zigzag black phosphorene nanotubes with approximately equal diameters. Young's modulus, critical stress and critical strain are estimated with various tube lengths. It is found that under uniaxial compression the (0, 24) armchair black phosphorene nanotube buckles, whereas the failure of the (31, 0) zigzag one is caused by local bond breaking near the boundary.

Keywords: atomistic simulation, compression, mechanical properties, phosphorene nanotubes.

1. INTRODUCTION

A black phosphorene nanotube (BPNT) can be viewed as rolling up a single-layer black phosphorene sheet along the armchair and zigzag direction as schematically shown in Fig. 1. The mechanical properties of black phosphorene have been investigated by density functional theory (DFT) calculations [1], molecular dynamics (MD) simulations [2–6], finite element analysis (FEA) with beam model [7] and density functional tight-binding (DF-TB) calculation [8]. The mechanical and electronic properties of monolayer and bilayer phosphorene have been recently studied by DFT calculations by Hu et al. [1]. Wang et al. [2] investigated the effects of mechanical strain on single-layer black phosphorene nanoresonators at different temperatures by MD simulation. The temperature-dependent stress-strain relations of black phosphorene under uniaxial tension are also investigated [3]. It was shown that the Young's moduli, fracture strength and strain slowly decrease with increasing the temperature [3, 4]. Chen et al. [5] performed MD simulations with compass force field and showed that Young's modulus of BPNT could increase with the tube length and diameter. Strength and stability of BPNT under axial compression has been recently investigated by MD simulation by Cai et al. [6]. It was shown that for an armchair tube with the same ratio of length over diameter, the critical strain decreases

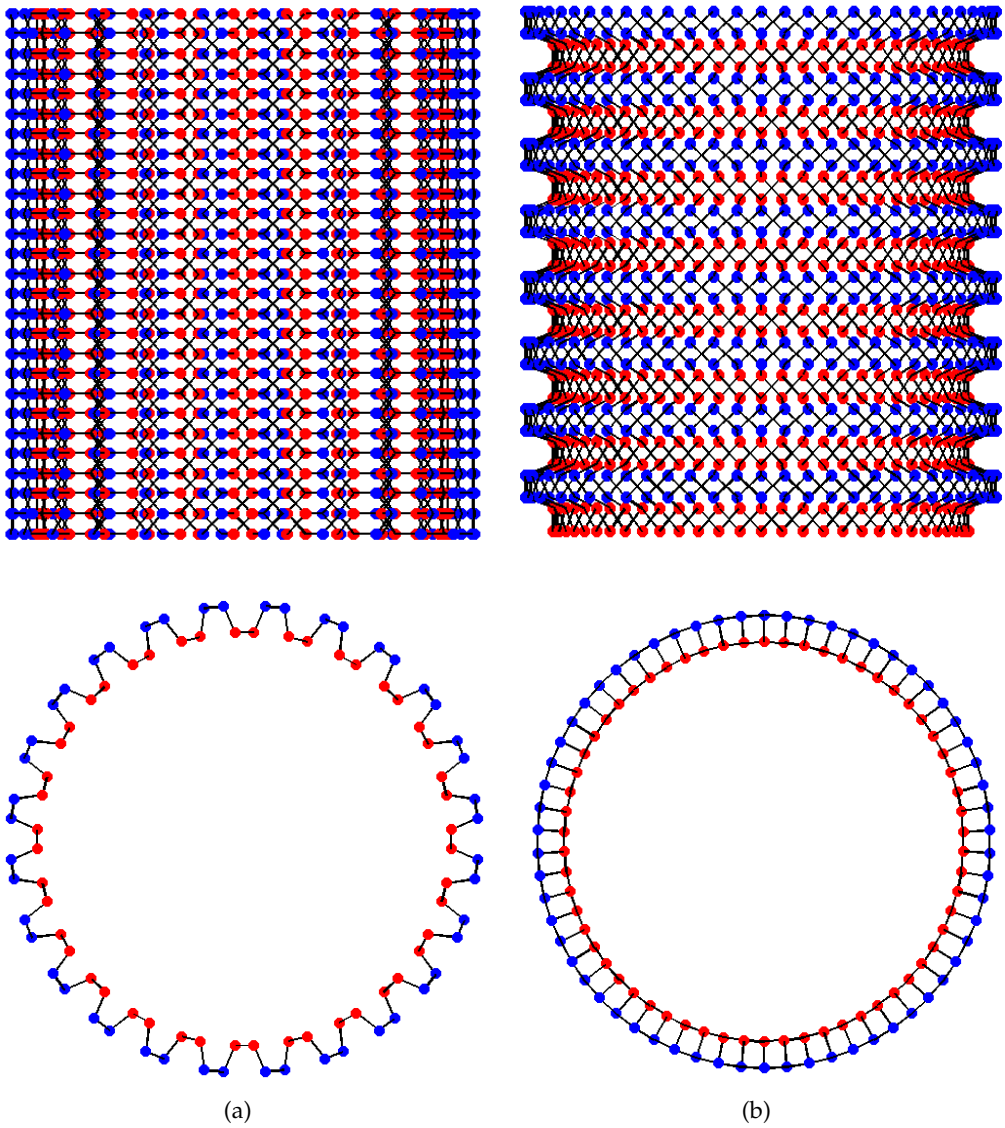

Fig. 1. Schematic illustration of: a) (0, 24) armchair black phosphorene nanotube; b) (31, 0) zigzag black phosphorene nanotube

with increasing the diameter and for an armchair tube with the same cross-section, the critical strain decreases with increasing its length. FEA with beam elements by Ansari et al. [7] revealed that phosphorene nanotubes with larger diameter have larger Young's modulus. Density functional theory (DFT)-tight binding calculations by Sorkin et al. [8] showed that fracture stress and Young's modulus of armchair BPNTs are larger than those of zigzag BPNTs.

In our previous work, the tensile response of 3 pairs of BPNTs was considered [9]. Here, we study the uniaxial compression of armchair and zigzag BPNTs with molecular dynamics finite element method (MDFEM) and Stillinger–Weber potential.

2. NUMERICAL PROCEDURE

The armchair (0, 24) BPNT with a diameter of 33,477 Å and zigzag (31, 0) tube with a diameter of 32,678 Å are studied. Tube lengths are $L = 60, 100$, and 140 Å. The geometric parameters of black phosphorene are used from reference [10].

Stillinger–Weber potential is used to model the interatomic interactions [11]. Numerical procedure of MDFEM with Stillinger–Weber potential was described in our previous work [12]. We also follow here similar notations as in our previous studies [9, 12].

3. RESULTS AND DISCUSSION

Fig. 2 shows the stress-strain curves of armchair and zigzag BPNTs under uniaxial compression. At a given axial compressive strain, the stress of the armchair BPNT is always higher than that of the corresponding zigzag one. The axial compressive stress increases monotonously with an increase of the axial compressive strain up to a peak value, then the axial compressive stress drops suddenly for all tubes as indicated in Fig. 2. Maximal axial stress and strain at maximal stress refer to critical stress and critical strain, respectively.

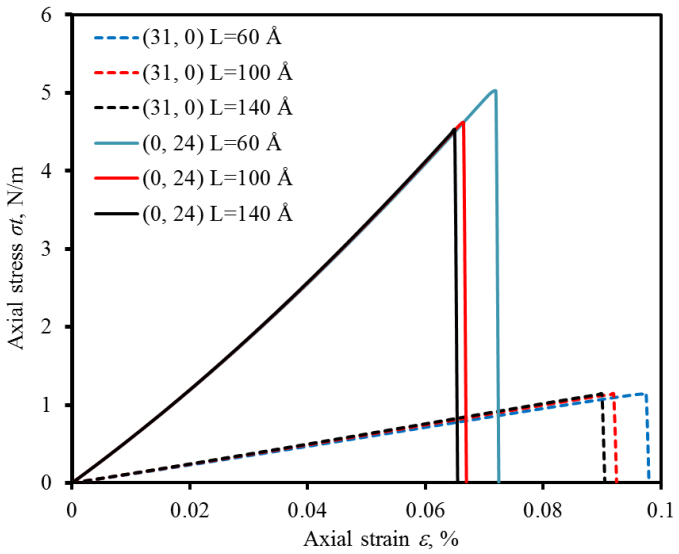

Fig. 2. The axial compressive stress-strain curves of armchair and zigzag black phosphorene nanotubes under uniaxial compression

Tab. 1 shows the Young's modulus, critical stress and critical strain of BPNTs. Results reveal that 2D critical stress of the armchair (0, 24) nanotube (4.617 N/m) is about four times larger than that of zigzag (31, 0) nanotube (1.142 N/m) with tube length $L = 100$ Å.

These results agree with those from DF-TB calculations of (0, 8) armchair and (8, 0) zigzag BPNTs [8] (the 2D critical stress of the armchair (0, 8) nanotube (13 GPa) is about three times larger than that of zigzag (8, 0) nanotube (4 GPa). In addition, the critical strain of the armchair (0, 24) and zigzag (31, 0) BPNTs is 6.65% and 9.20%, with $L = 100$ Å, respectively. When $L = 100$ Å, the 2D Young's modulus is ~ 55 N/m for the armchair (0, 24) BPNT, and ~ 11.7 N/m for the zigzag (31, 0) one.

Table 1. The mechanical properties of (0, 24) armchair and (31, 0) zigzag BPNTs

Tubes	Young's modulus Yt, N/m	Critical stress σt, N/m	Critical strain ε, %
Armchair (0, 24)			
$L = 60$ Å	54.85	5.022	7.20
$L = 100$ Å	55.03	4.617	6.65
$L = 140$ Å	55.10	4.528	6.50
Zigzag (31, 0)			
$L = 60$ Å	11.33	1.151	9.25
$L = 100$ Å	11.71	1.142	9.20
$L = 140$Å	11.88	1.139	9.00

Table 2. 2D Young's modulus of black phosphorene sheet and tubes by various methods

References	Types	Young's modulus Yt, N/m
Present study by MDFEM calculations	Armchair tube	55.03
	Zigzag tube	11.71
Wang et al. [2] by MD simulations	Zigzag direction, sheet	55.5
	Armchair direction, sheet	13.6
Cai et al. [6] by MD simulations	Zigzag tube	10.29
Ansari et al. [7] by DFT-FEM calculations	Zigzag tube	14.67
Sorkin et al. [8] by DF-TB calculations	Armchair tube	27.12
	Zigzag tube	10.65

Tab. 2 shows the Young's modulus of black phosphorene sheet and tubes from various methods. Results reveal that the 2D Young's modulus of zigzag phosphorene tube (~ 11.7 N/m) is close to that from FEA for (24, 0) zigzag BPNT 14.67 N/m [7], from MD simulations of (14, 0) zigzag BPNT 48.255 GPa (~ 10.29 N.m) [6] and from DF-TB calculations of (24, 0) zigzag BPNT 45 GPa (2D Young's modulus $Yt \sim 10.65$ N/m) [8]. The

2D Young's modulus of the armchair nanotube ($\sim$ 55 N/m) is higer than that from DF-TB calculations 114.2 GPa (2D Young's modulus $Yt \sim 27.12$ N/m) [8]. Critical stress and critical strain of armchair and zigzag BPNTs decrease with an increase of length-diameter ratio L/D as shown in Figs. 3 and 4.

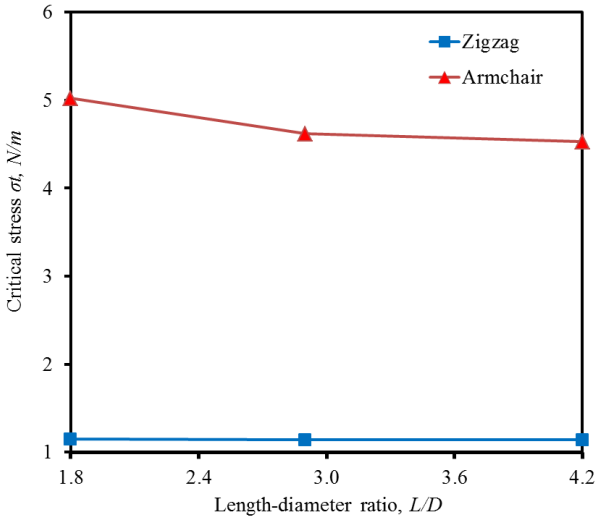

Fig. 3. Variations of the critical stress versus the L/D ratio of armchair and zigzag black phosphorene nanotubes under uniaxial compression

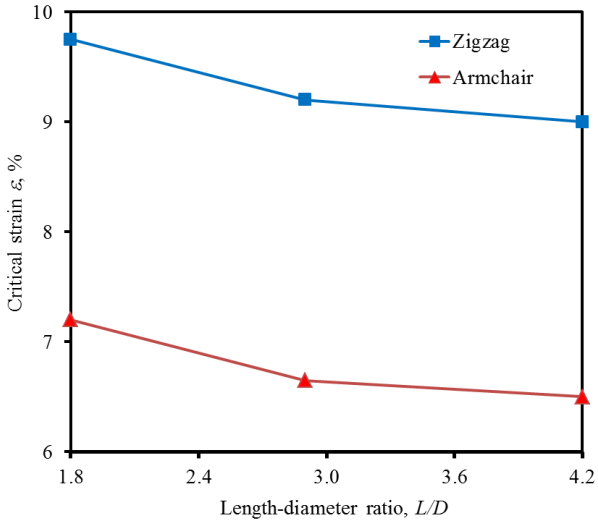

Fig. 4. Variations of the critical strain versus the L/D ratio of armchair and zigzag black phosphorene nanotubes under uniaxial compression

Figs. 5 and 6 show the snapshots of (0, 24) armchair and (31, 0) zigzag BPNTs under uniaxial compression, respectively. The (0, 24) armchair nanotube exhibits clearly

buckling under uniaxial compression when its compressive axial strain exceeds a critical value of $\sim$ 6.60%. In the other hand, buckling is not observed for the (31, 0) zigzag one under compression. The failure of this tube is caused by local bond breaking near the boundary. The puckers are parallel to the armchair direction, which is the direction of tube axis (the compressive direction) of the (0, 24) armchair tube as indicated in Fig. 1(a). Whereas, the compressive direction (the tube axis) of the (31, 0) zigzag tube is perpendicular to the plans of puckers as shown in Fig. 1(b). These crystal structures lead to the fact that the Young's modulus and critical stress of the armchair tube are higher than those of the zigzag one, while the critical strain of the armchair tube is lower than that of the zigzag one as shown in Fig. 2 and Tab. 1.

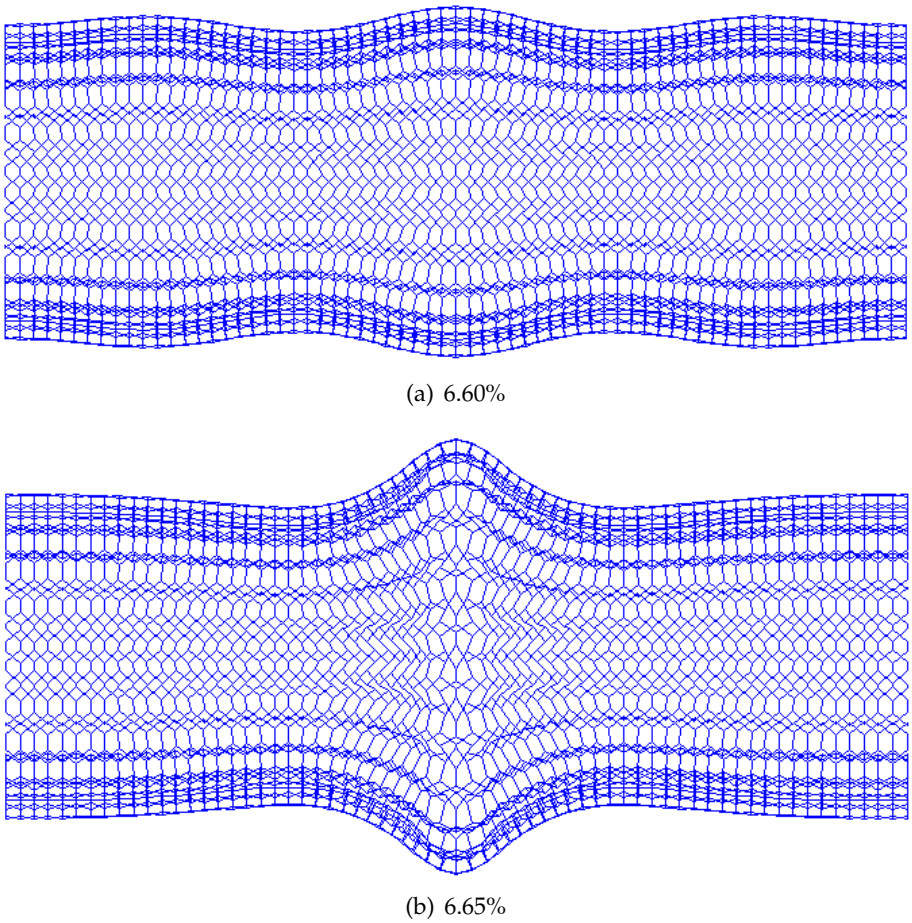

(a) 6.60%

(b) 6.65%

Fig. 5. Snapshots of (0, 24) armchair black phosphorene nanotube ($L = 100$ Å) at an axial compressive strain of: a) $\varepsilon = 6.60\%$; and b) $\varepsilon = 6.65\%$

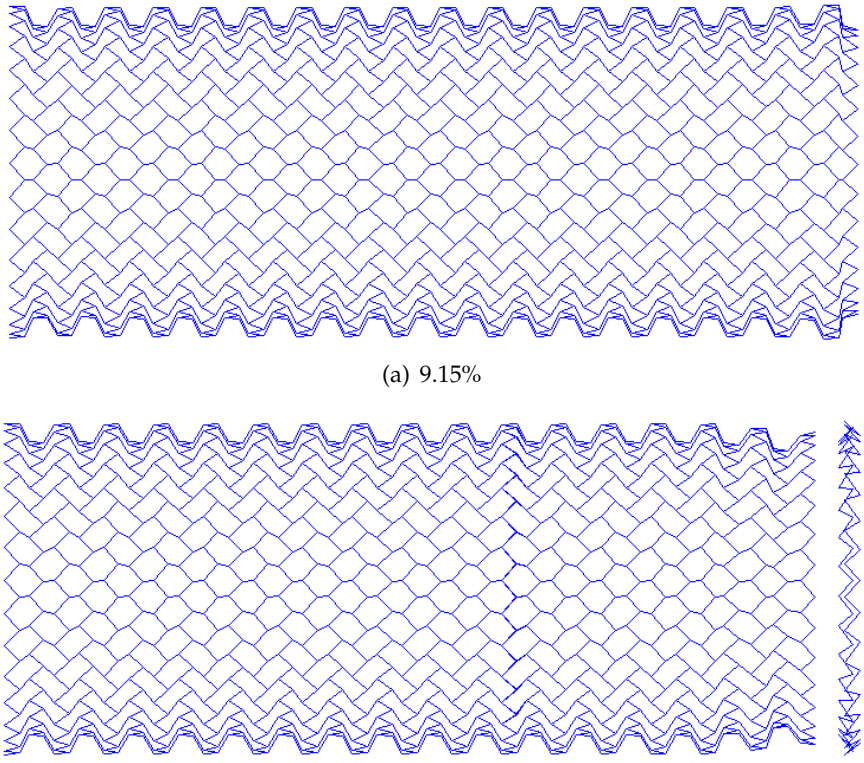

(a) 9.15%

(b) 9.20%

Fig. 6. Snapshots of (31, 0) zigzag black phosphorene nanotube ($L = 100$ Å) at an axial compressive strain of: a) $\varepsilon = 9.15\%$; and b) $\varepsilon = 9.20\%$

4. CONCLUSIONS

The present work uses MDFEM with Stillinger–Weber potential to study the compressive behavior of (0, 24) armchair and (31, 0) zigzag BPNTs. The (0, 24) armchair nanotube exhibits clearly buckling under uniaxial compression. The failure of the (31, 0) zigzag one under compression is caused by local bond breaking near the boundary. Young's modulus and critical stress of the armchair tube are higher than those of the corresponding zigzag one, while an inverse trend is found for the critical strain. Critical stress and critical strain decrease with an increase of length-diameter ratio L/D. The mechanical behavior of these two tubes under compression are highly different from each other although their diameters are approximately equal. These issues should be further studied to get more information for the design and application of BPNTs in nanodevices.

ACKNOWLEDGMENT

This work was supported by Vietnam National Foundation for Science and Technology Development (NAFOSTED) under the grant number: 107.02-2017.02.

REFERENCES

[1] T. Hu, Y. Han, and J. Dong. Mechanical and electronic properties of monolayer and bilayer phosphorene under uniaxial and isotropic strains. *Nanotechnology*, **25**, (45), (2014). https://doi.org/10.1088/0957-4484/25/45/455703.

[2] C.-X. Wang, C. Zhang, J.-W. Jiang, H. S. Park, and T. Rabczuk. Mechanical strain effects on black phosphorus nanoresonators. *Nanoscale*, **8**, (2), (2016), pp. 901–905. https://doi.org/10.1039/c5nr06441d.

[3] Z.-D. Sha, Q.-X. Pei, Z. Ding, J.-W. Jiang, and Y.-W. Zhang. Mechanical properties and fracture behavior of single-layer phosphorene at finite temperatures. *Journal of Physics D: Applied Physics*, **48**, (39), (2015). https://doi.org/10.1088/0022-3727/48/39/395303.

[4] Z. Yang, J. Zhao, and N. Wei. Temperature-dependent mechanical properties of monolayer black phosphorus by molecular dynamics simulations. *Applied Physics Letters*, **107**, (2), (2015). https://doi.org/10.1063/1.4926929.

[5] W.-H. Chen, C.-F. Yu, I.-C. Chen, and H.-C. Cheng. Mechanical property assessment of black phosphorene nanotube using molecular dynamics simulation. *Computational Materials Science*, **133**, (2017), pp. 35–44. https://doi.org/10.1016/j.commatsci.2017.03.008.

[6] K. Cai, J. Wan, N. Wei, and Q. H. Qin. Strength and stability analysis of a single-walled black phosphorus tube under axial compression. *Nanotechnology*, **27**, (27), (2016). https://doi.org/10.1088/0957-4484/27/27/275701.

[7] R. Ansari, A. Shahnazari, and S. Rouhi. A density-functional-theory-based finite element model to study the mechanical properties of zigzag phosphorene nanotubes. *Physica E: Low-dimensional Systems and Nanostructures*, **88**, (2017), pp. 272–278. https://doi.org/10.1016/j.physe.2017.01.022.

[8] V. Sorkin and Y. Zhang. Mechanical properties of phosphorene nanotubes: a density functional tight-binding study. *Nanotechnology*, **27**, (39), (2016). https://doi.org/10.1088/0957-4484/27/39/395701.

[9] V.-T. Nguyen, D.-T. Nguyen, and M.-Q. Le. Atomistic simulation of the uniaxial tension of black phosphorene nanotubes. *Vietnam Journal of Mechanics*, **40**, (2), (2018), pp. 163–169. https://doi.org/10.15625/0866-7136/10751.

[10] Y. Takao, H. Asahina, and A. Morita. Electronic structure of black phosphorus in tight binding approach. *Journal of the Physical Society of Japan*, **50**, (10), (1981), pp. 3362–3369. https://doi.org/10.1143/jpsj.50.3362.

[11] J.-W. Jiang. Parametrization of Stillinger–Weber potential based on valence force field model: application to single-layer MoS2 and black phosphorus. *Nanotechnology*, **26**, (31), (2015). https://doi.org/10.1088/0957-4484/26/31/315706.

[12] D.-T. Nguyen, M.-Q. Le, V.-T. Nguyen, and T.-L. Bui. Effects of various defects on the mechanical properties of black phosphorene. *Superlattices and Microstructures*, **112**, (2017), pp. 186–199. https://doi.org/10.1016/j.spmi.2017.09.021.